

Shimokawa Y., Kikura-Hanajiri R., Aritake K.,
Urade Y., Goda Y.: Characterization of four
new designer drugs, 5-chloro-NNEI, NNEI
indazole analog, α -PHPP and α -POP, with 11
newly distributed designer drugs in illegal
products. *Forensic Sci. Int.*, (2014) 243, 1-13.

4. Uchiyama N., Shimokawa Y., Matsuda S.,
Kawamura M., Kikura-Hanajiri R., Goda Y.:
Two new synthetic cannabinoids, AM-2201
benzimidazole analog (FUBIMINA) and
(4-methylpiperazin-1-yl)
(1-pentyl-1H-indol-3-yl)methanone
(MEPIRAPIM), and three phenethylamine
derivatives, 25H-NBOMe
3,4,5-trimethoxybenzyl analog, 25B-NBOMe,
and 2C-N-NBOMe, identified in illegal
products identified in illegal products. *Forensic
Toxicol.* (2013) 32, 105–117.
5. 内山奈穂子: 違法ドラッグ (脱法ドラッグ)
の正体は? 和漢薬, 723, 10-11 (2013).

H. 知的財産権の出願・登録状況
特になし.

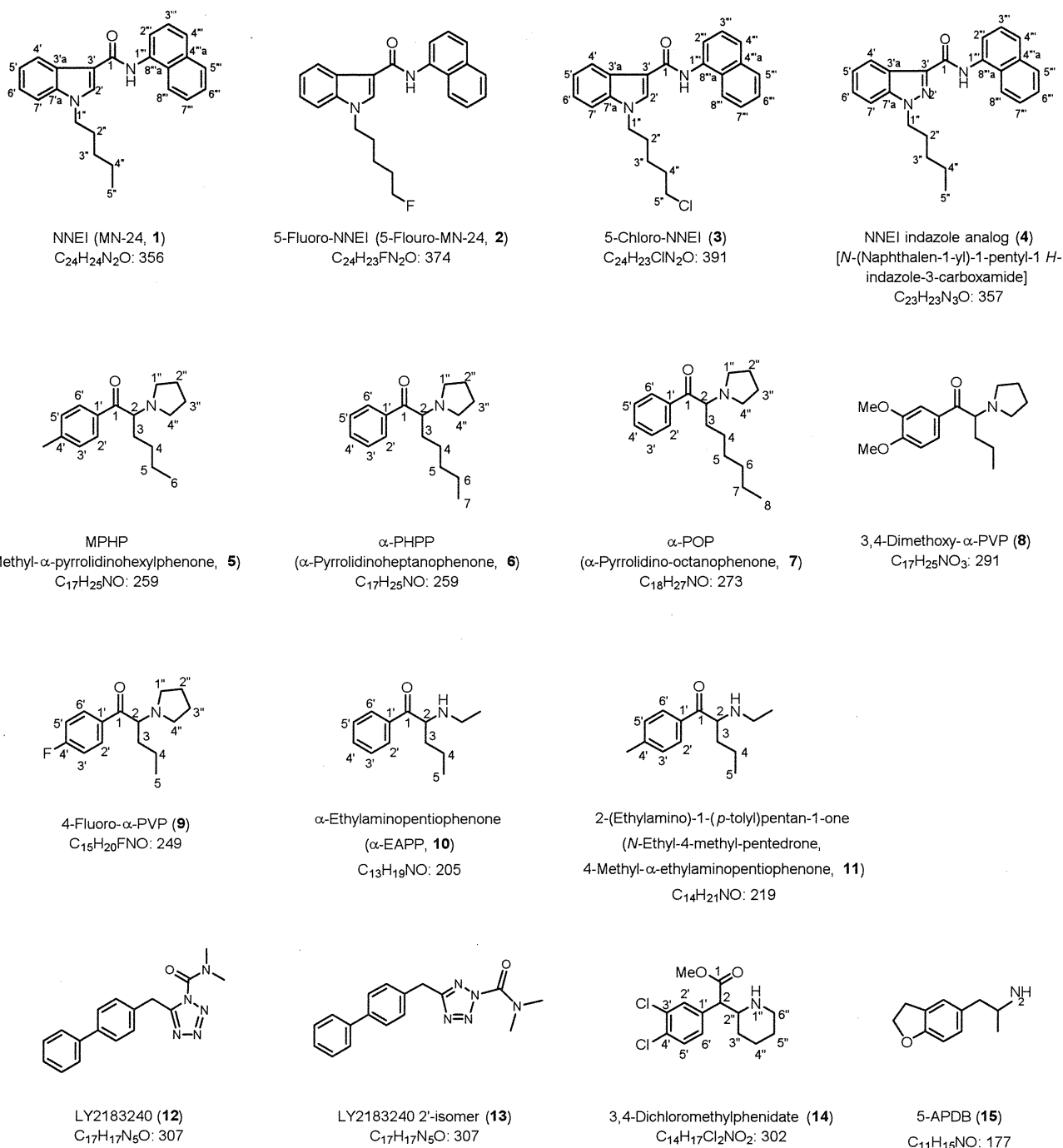
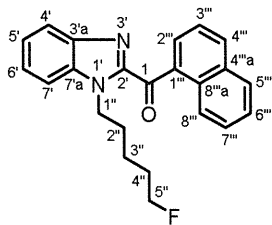
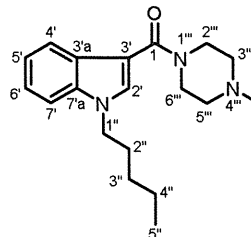


Fig. 1a. 平成 25 年度前半買い上げ違法ドラッグ製品より検出された新規流通化合物(1-15)

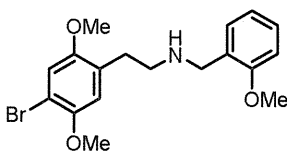
合成カンナビノイド(1-4), カチン系化合物(5-11), 合成カンナビノイド関連化合物(12, 13), その他化合物(14) 及びフェネチルアミン系化合物(15)



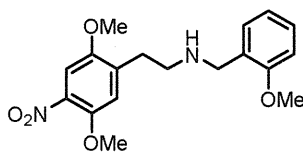
AM-2201 benzimidazole analog
(FUBIMINA, **16**)
(1-(5-Fluoropentyl)-1*H*-benzo[d]imidazol-2-yl)(naphthalen-1-yl)methanone
 $C_{23}H_{21}FN_2O$: 360



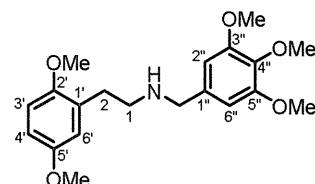
(4-Methylpiperazin-1-yl)(1-pentyl-1*H*-indol-3-yl)methanone
(MEPIRAPIM, **17**)
 $C_{19}H_{27}N_3O$: 313



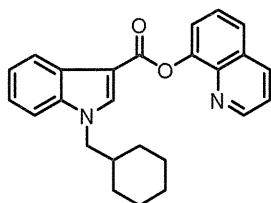
25B-NBOMe (**18**)
 $C_{18}H_{22}BrNO_3$: 380



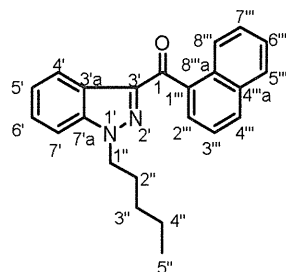
2C-N-NBOMe (**19**)
 $C_{18}H_{22}N_2O_5$: 346



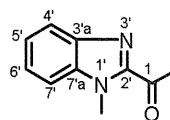
25H-NBOMe 3,4,5-trimethoxybenzyl analog (**20**)
[2-(2,5-Dimethoxyphenyl)-*N*-(3,4,5-trimethoxybenzyl)ethanamine]
 $C_{20}H_{27}NO_5$: 361



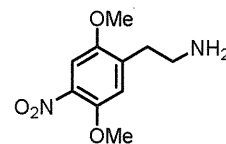
QUCHIC (BB-22)
 $C_{25}H_{24}N_2O_2$: 384



JWH-018 indazole analog
 $C_{23}H_{22}N_2O$: 342



2-Acetyl-1-methyl-1*H*-benzimidazole



2C-N

Fig. 1b. 平成 25 年度前半買上げ違法ドラッグ製品より検出された新規流通化合物 (**16–20**)

合成カンナビノイド (**16, 17**), フェネチルアミン系化合物 (**18–20**) 及び関連化合物

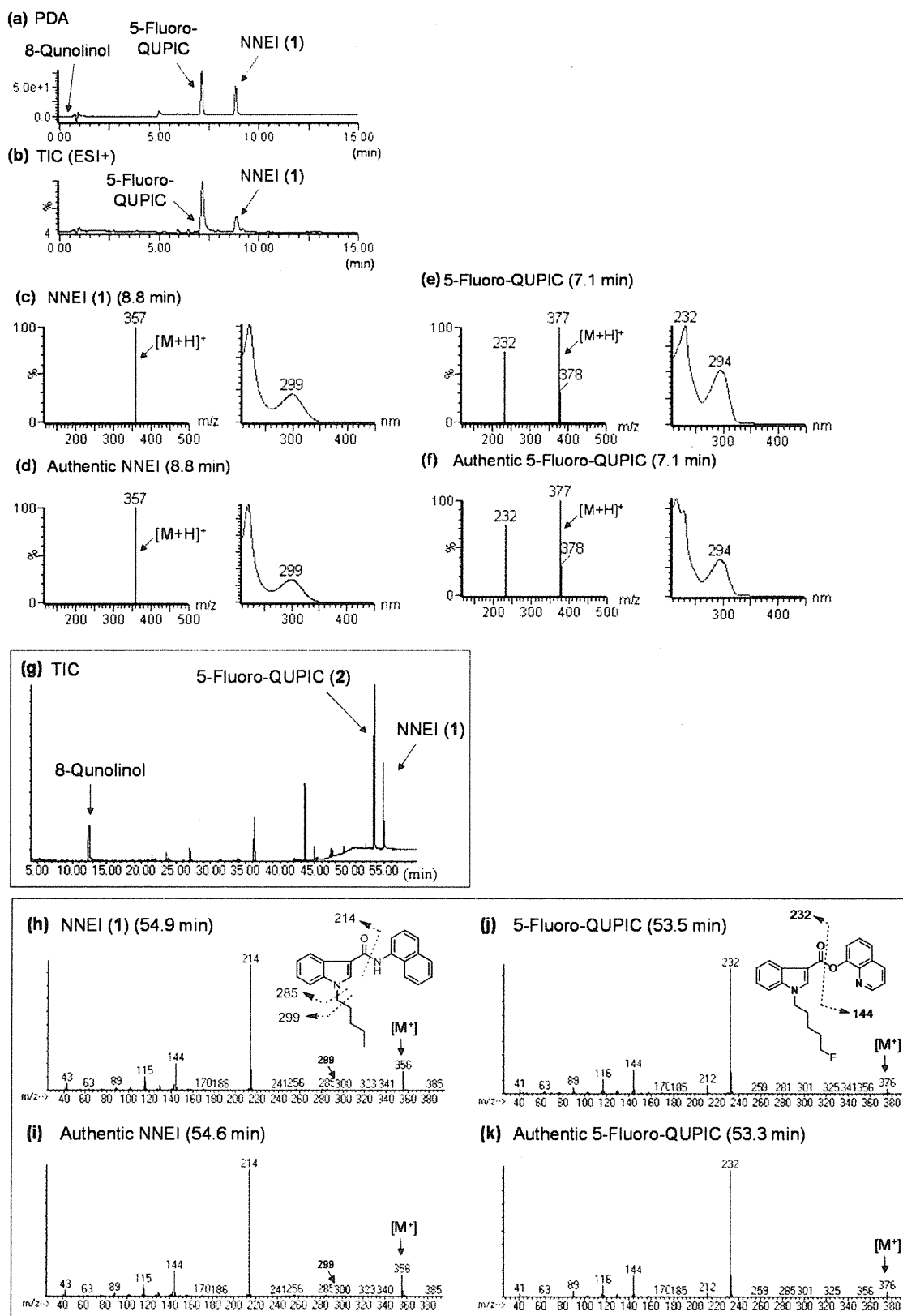


Fig. 2. LC-MS and GC-MS analyses of product A. LC-UV-PDA chromatogram (a) and total ion chromatogram (TIC) (b). ESI mass and UV spectra of peaks 1 (c), 5-fluoro-QUPIC (e), authentic NNEI and 5-fluoro-QUPIC (d and f, respectively). TIC (g) and EI mass spectra of peaks 1 (h), 5-fluoro-QUPIC (j) and authentic NNEI and 5-fluoro-QUPIC (i and k, respectively) obtained by GC-MS analysis.

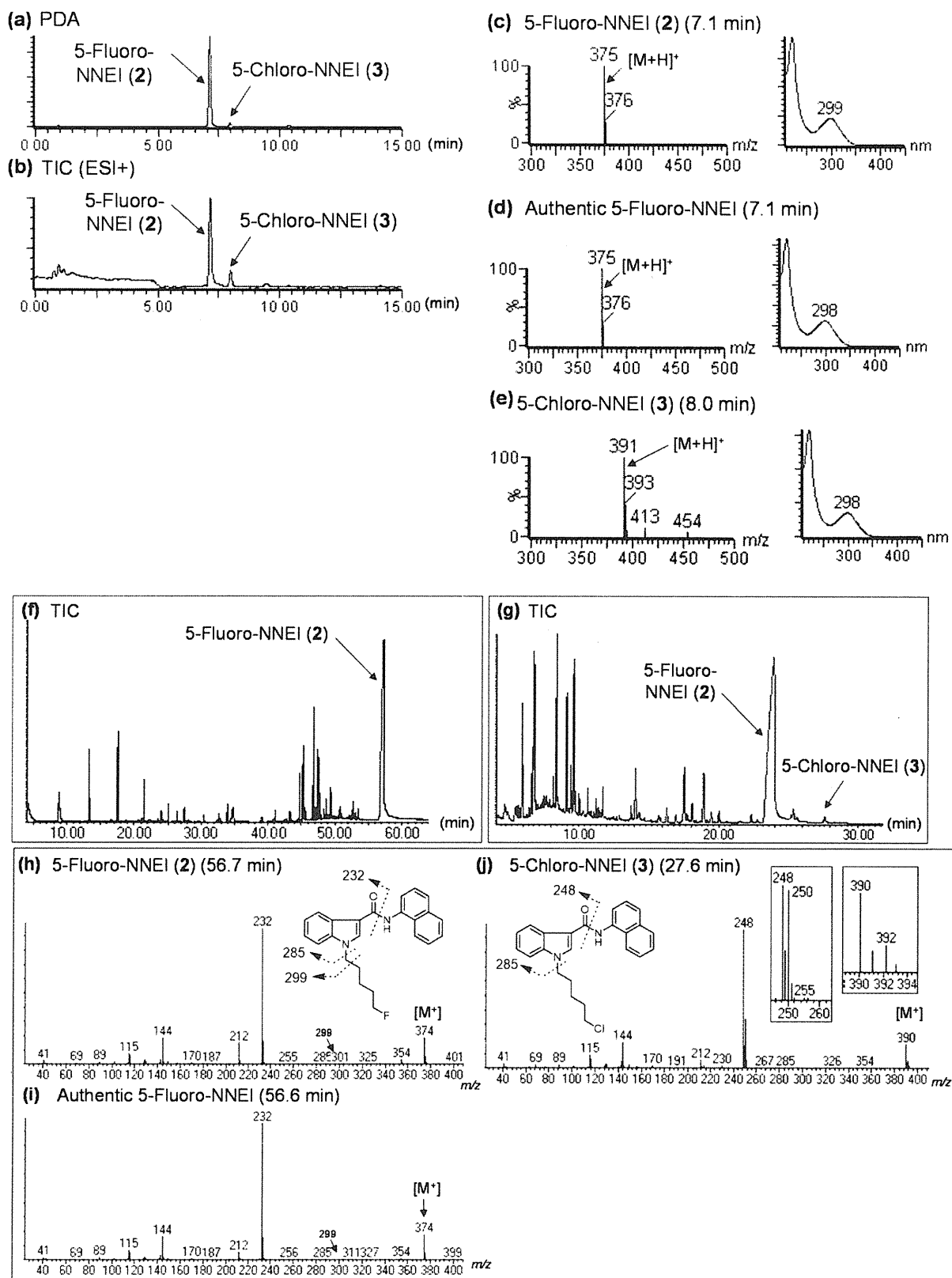
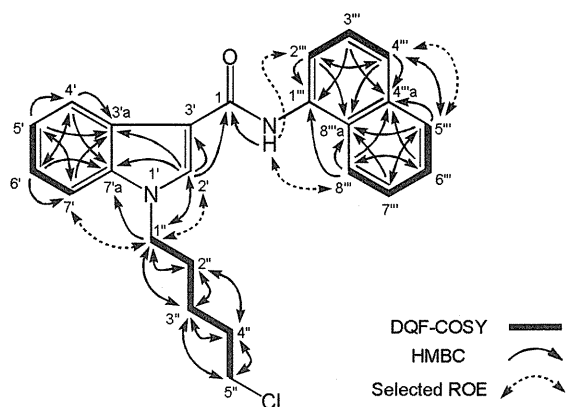
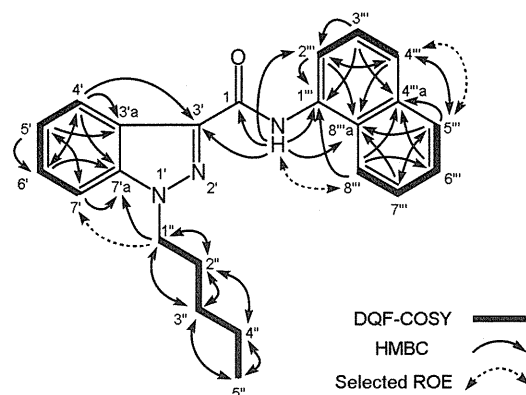


Fig. 3. LC-MS and GC-MS analyses of product B. LC-UV-PDA chromatogram (a) and TIC (b). ESI mass and UV spectra of peaks 2 (c), 3 (e) and authentic 5-fluoro-NNEI (d). TIC (f, g) and EI mass spectra of peaks 2 (h), 3 (j) and authentic 5-fluoro-NNEI (i) obtained by the GC-MS analysis.

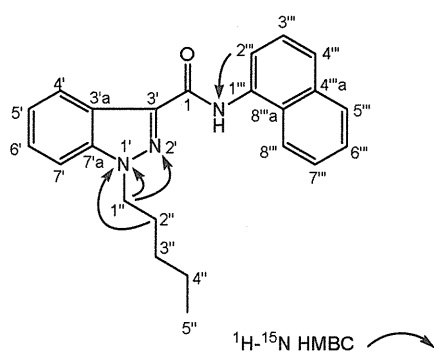
(a) 5-Chloro-NNEI (3)



(b) NNEI indazole analog (4)



(c) NNEI indazole analog (4)



(d) 3,4-Dichloromethylphenidate (14)

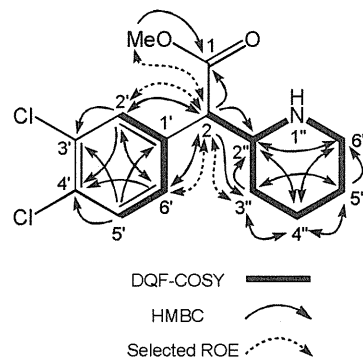


Fig. 4. DQF-COSY, selected HMBC, and selected ROE correlations (a) for compound 3 (5-chloro-NNEI), and DQF-COSY, selected HMBC and selected ROE correlations for compound 4 (NNEI indazole analog, b) and compound 14 (3,4-Dichloromethylphenidate, d). ^1H - ^{15}N HMBC correlation for compound 4 (NNEI indazole analog, c).

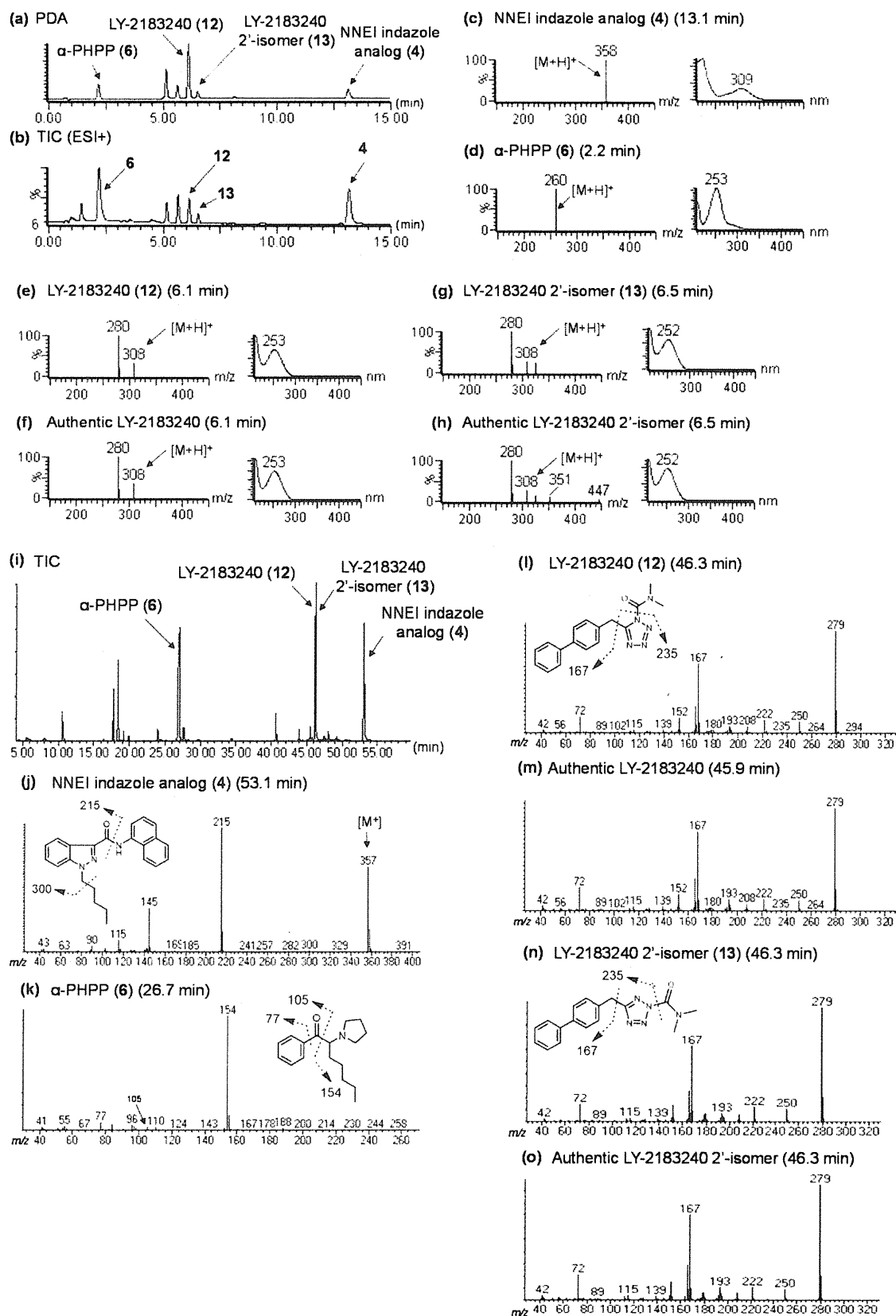


Fig. 5. LC-MS and GC-MS analyses of product C. LC-UV-PDA chromatogram (a) and TIC (b). ESI mass and UV spectra of peaks 4 (c), 6 (d), 12 (e), 13 (g) and authentic LY-2183240 and LY-2183240 2'-isomer (f and h), respectively. TIC (i) and EI mass spectra of peaks 4 (i), 6 (k), 12 (l), 13 (m) and authentic LY-2183240 and LY-2183240 2'-isomer (n and o), respectively, obtained by the GC-MS analysis.

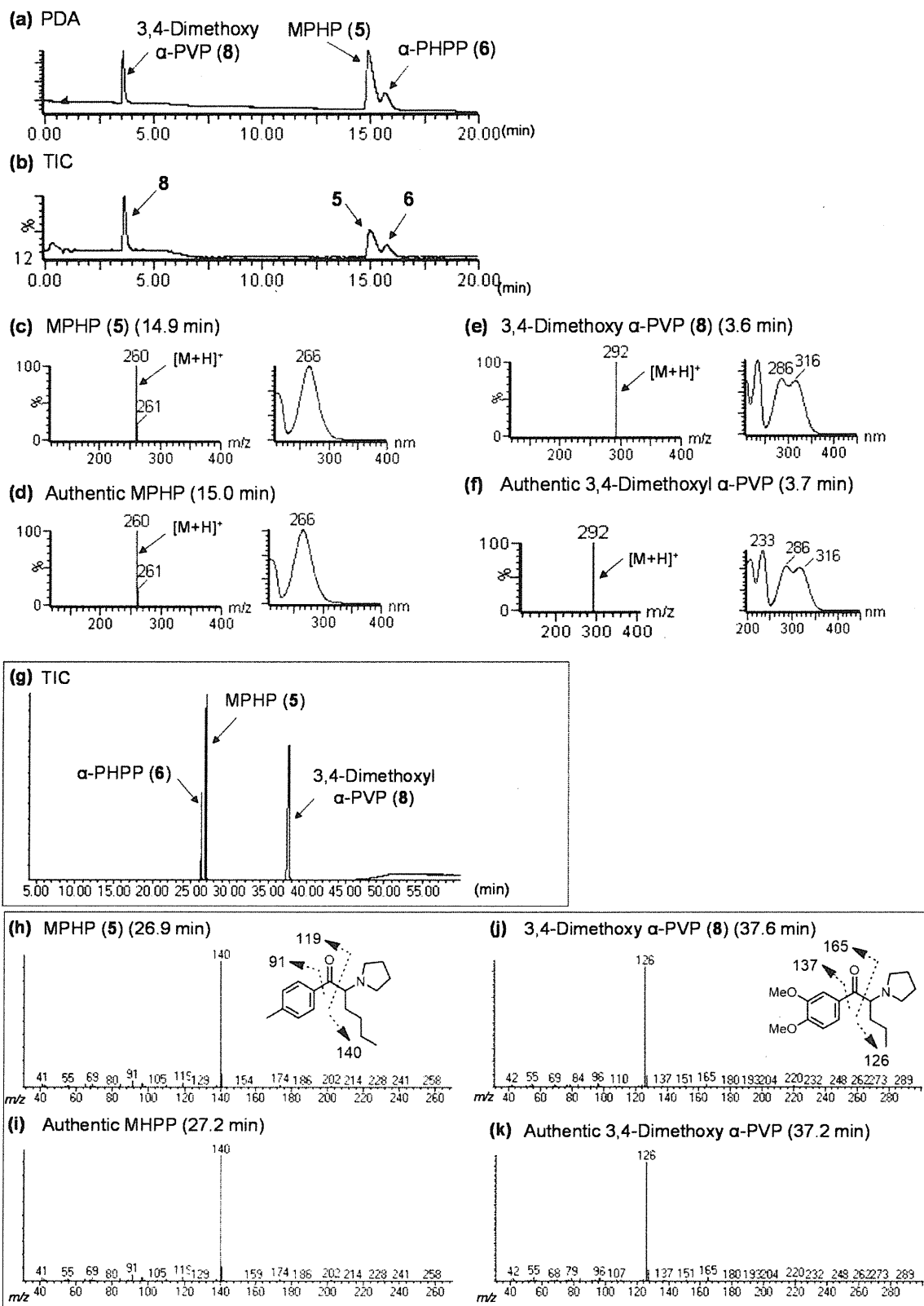


Fig. 6. LC-MS and GC-MS analyses of product D. LC-UV-PDA chromatogram (a) and TIC (b). ESI mass and UV spectra of peaks 5 (c), 8 (e) and authentic MPHP and 3,4-dimethoxy- α -PVP (d and f), respectively. TIC (g) and EI mass spectra of peaks 5 (h), 8 (j) and authentic MPHP and 3,4-dimethoxy- α -PVP (i and k), respectively, obtained by the GC-MS analysis.

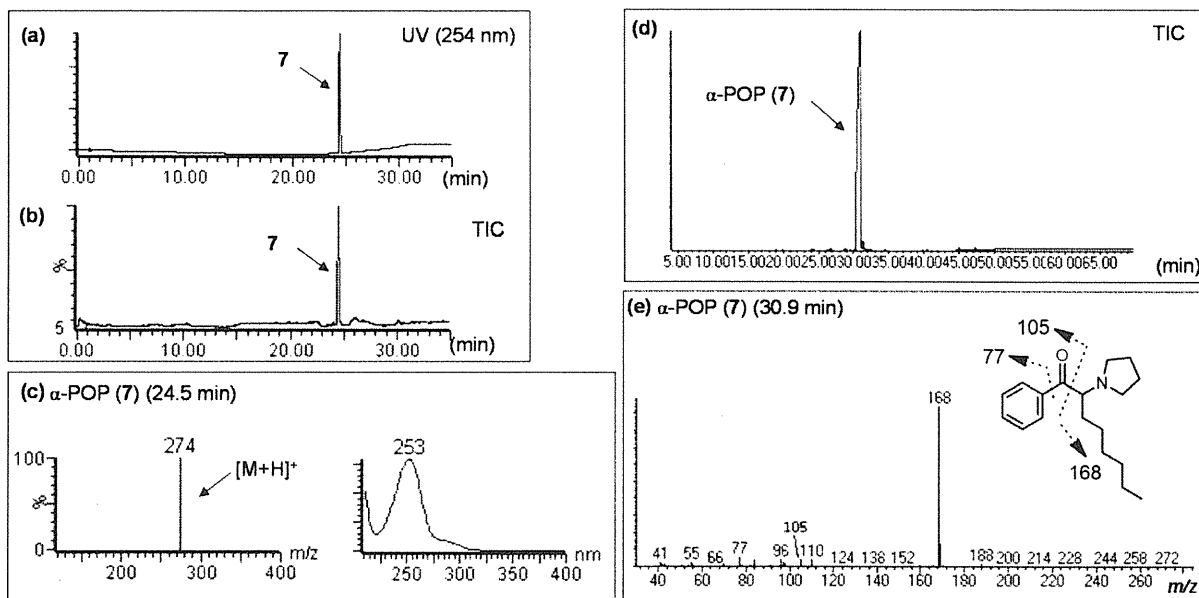


Fig. 7. LC-MS and GC-MS analyses of product E. LC-UV-PDA chromatogram (a), TIC (b) and ESI mass and UV spectra of peak 7 (c). TIC (d) and EI mass spectrum of peak 7 (e) obtained by the GC-MS analysis.

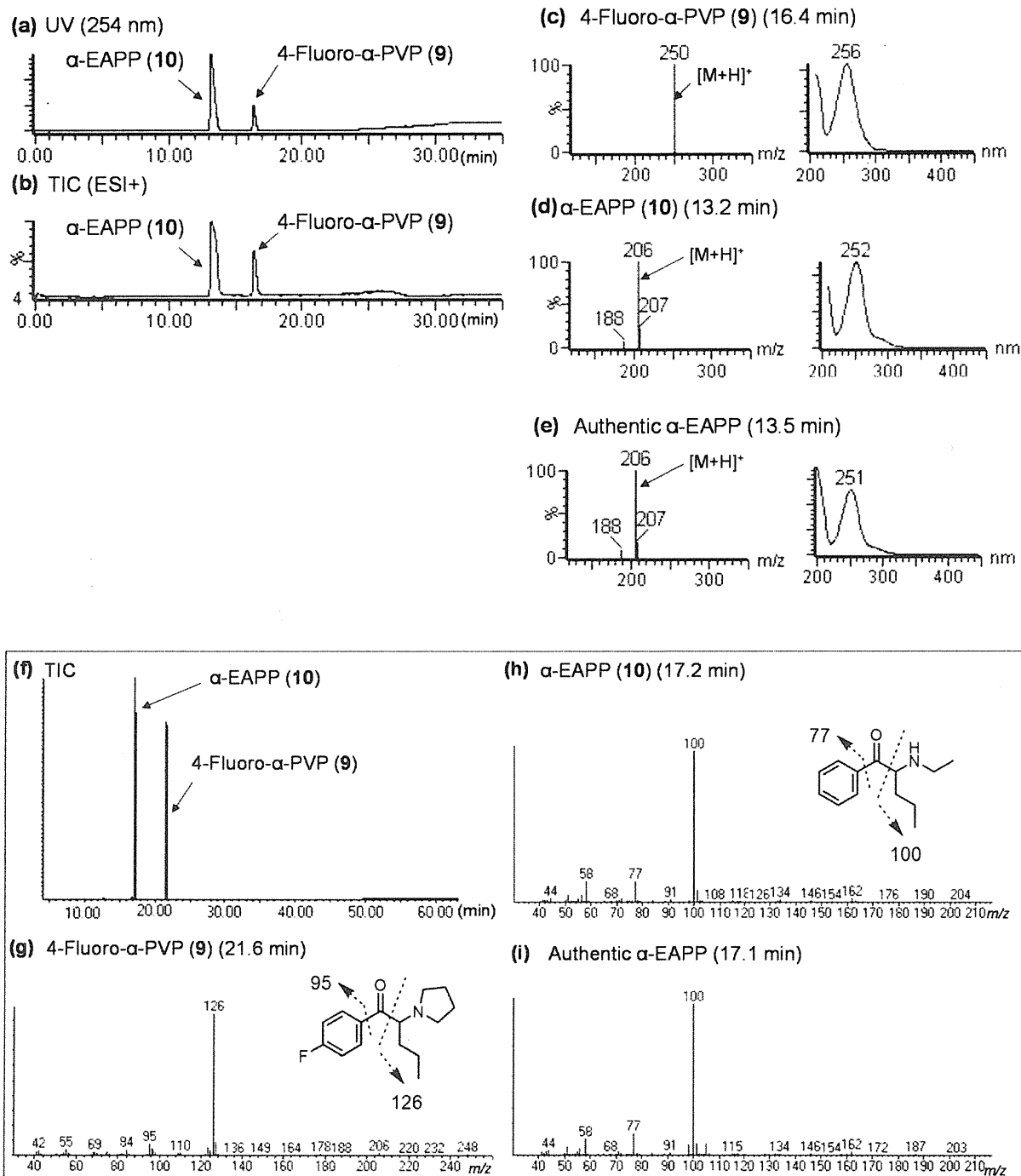


Fig. 8. LC-MS and GC-MS analyses of product F. LC-UV-PDA chromatogram (a) and TIC (b). ESI mass and UV spectra of peaks 9 (c), 10 (d) and authentic α -EAHP (e), respectively. TIC (f) and EI mass spectra of peaks 9 (g), 10 (h) and authentic α -EAHP (i), respectively, obtained by the GC-MS analysis.

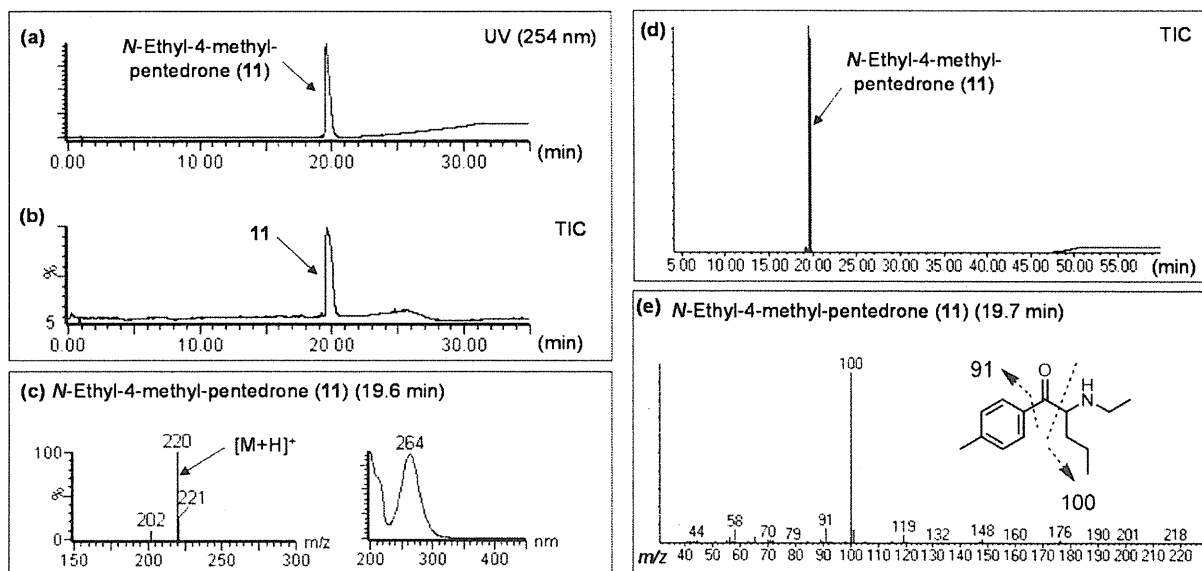


Fig. 9. LC-MS and GC-MS analyses of product G. LC-UV-PDA chromatogram (a), TIC (b) and ESI mass and UV spectra of peak 11 (c). TIC (d) and EI mass spectrum of peak 11 (e) obtained by the GC-MS analysis.

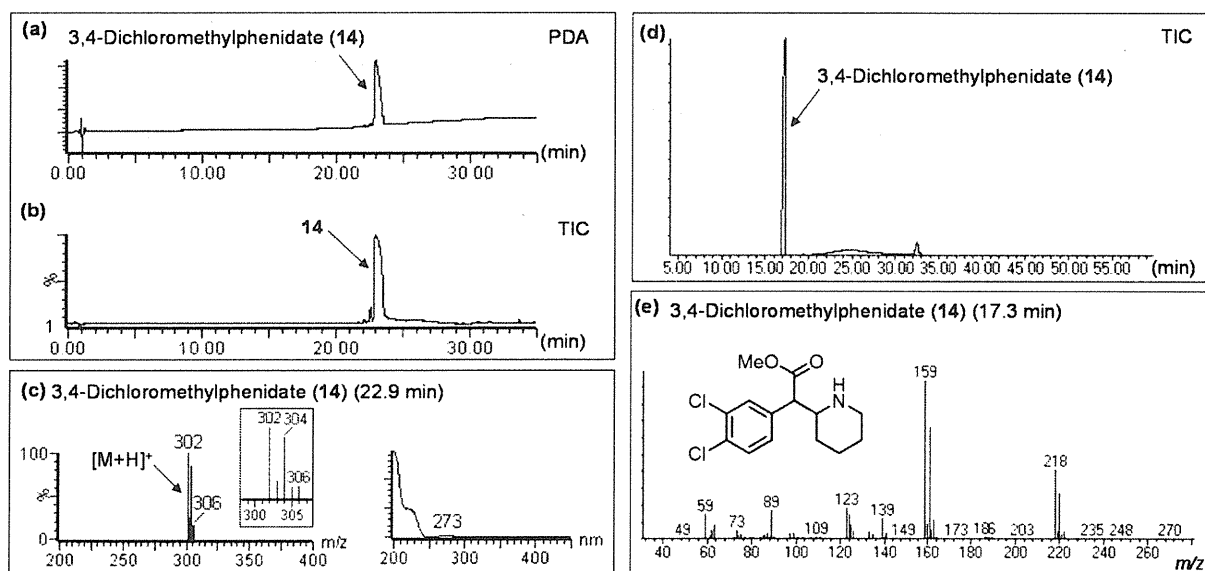


Fig. 10. LC-MS and GC-MS analyses of product H. LC-UV-PDA chromatogram (a), TIC (b) and ESI mass and UV spectra of peak 14 (c). TIC (d) and EI mass spectrum of peak 14 (e) obtained by the GC-MS analysis.

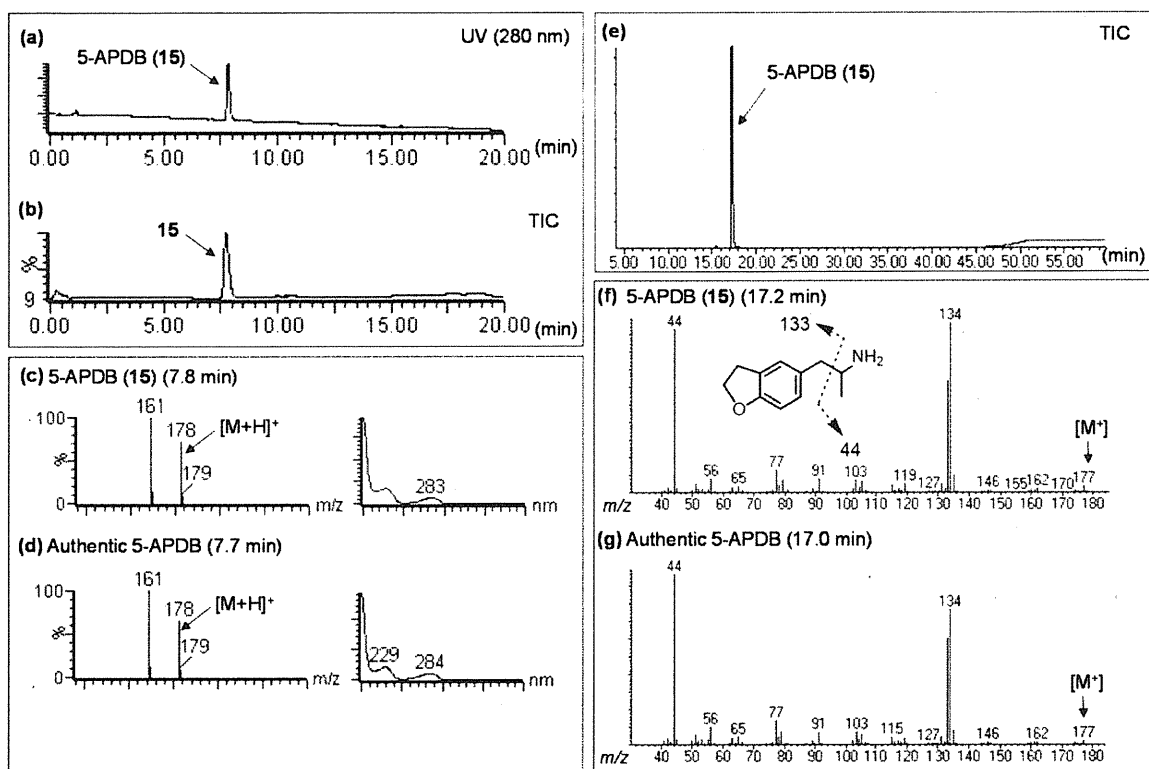


Fig. 11. LC-MS and GC-MS analyses of product I. LC-UV-PDA chromatogram (a) and TIC (b). ESI mass and UV spectra of peaks 15 (c) and authentic 5-APDB (d), respectively. TIC (e) and EI mass spectra of peaks 15 (f) and authentic 5-APDB (g), respectively, obtained by the GC-MS analysis.

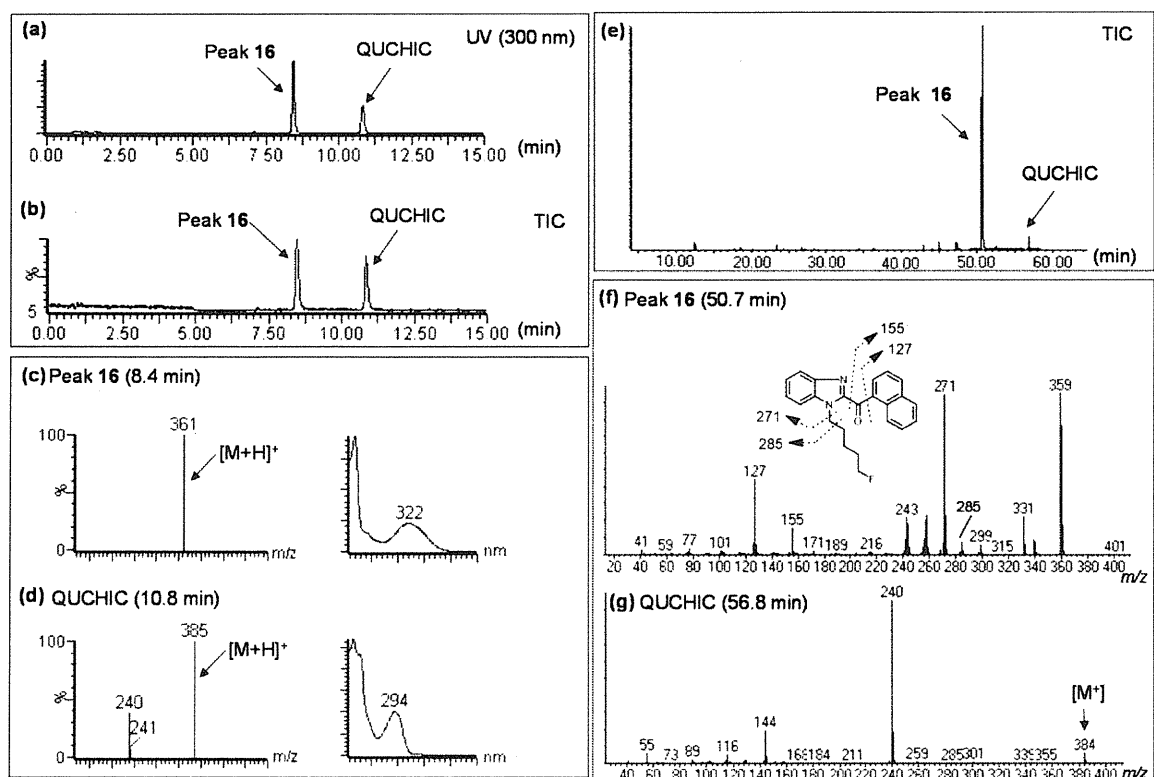
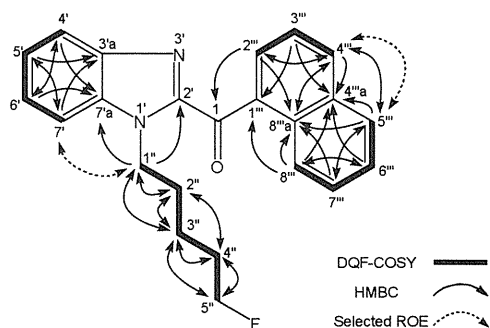
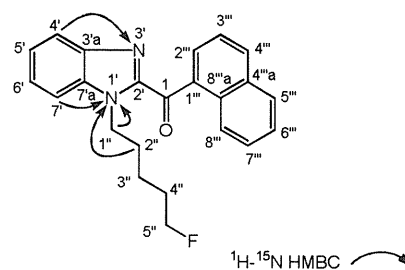


Fig. 12. LC-MS and GC-MS analyses of product J. LC-UV-PDA chromatogram (a) and total ion chromatogram (TIC) (b). ESI mass and UV spectra of peaks 16 (c) and QUCHIC (d). TIC (e) and EI mass spectra of peaks 16 (f) and QUCHIC (g) obtained by GC-MS analysis.

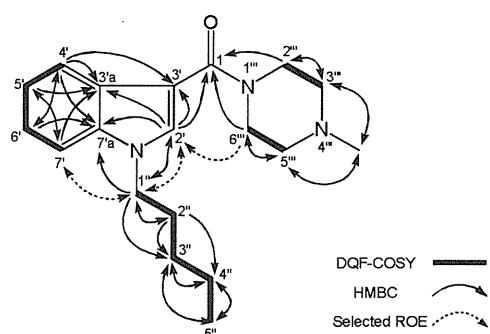
(a) AM-2201 benzimidazole analog (16)



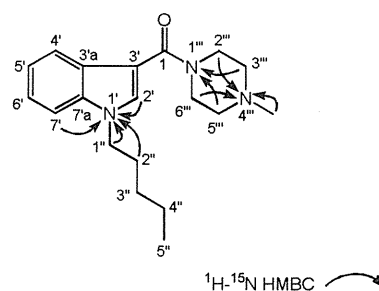
(b) AM-2201 benzimidazole analog (16)



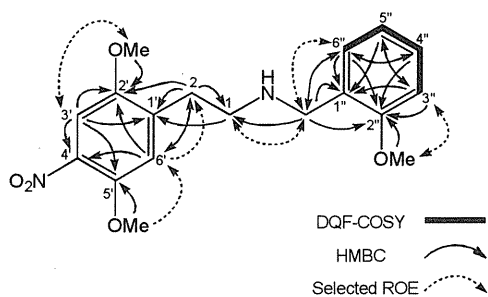
(c) (4-methylpiperazin-1-yl)(1-pentyl-1*H*-indol-3-yl)methanone (17)



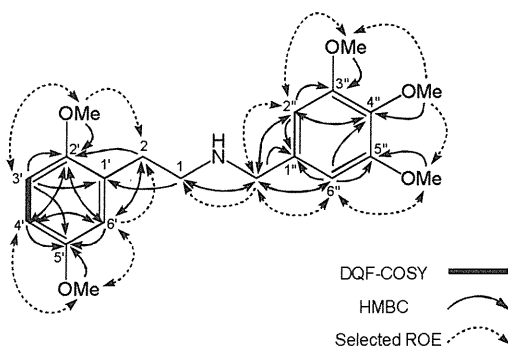
(d) (4-methylpiperazin-1-yl)(1-pentyl-1*H*-indol-3-yl)methanone (17)



(e) 2*C*-*N*-NBOMe (19)



(f) 2-(2,5-Dimethoxyphenyl)-*N*-(3,4,5-trimethoxybenzyl)ethanamine (20)



(g) 2-(2,5-Dimethoxyphenyl)-*N*-(3,4,5-trimethoxybenzyl)ethanamine (20)

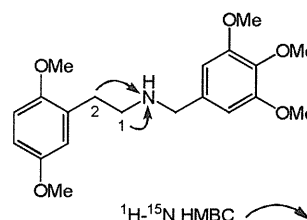


Fig. 13. DQF-COSY, selected HMBC, and selected ROE correlations for compounds 16 (a), 17 (c), 19 (e) and 20 (f), and ^1H - ^{15}N HMBC correlations for compounds 16 (b), 17 (d), and 20 (g), respectively.

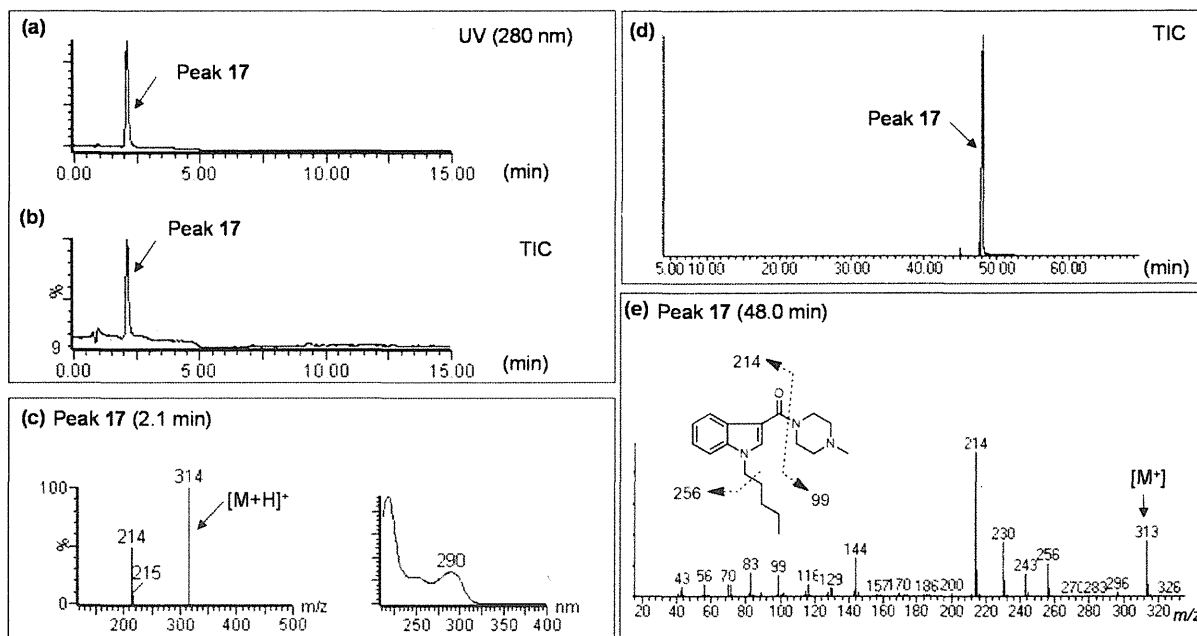


Fig. 14. LC-MS and GC-MS analyses of product K. LC-UV-PDA chromatogram (a) and TIC (b). ESI mass and UV spectra of peak 17 (c). TIC (d) and EI mass spectrum of peak 17 (e) obtained by the GC-MS analysis.

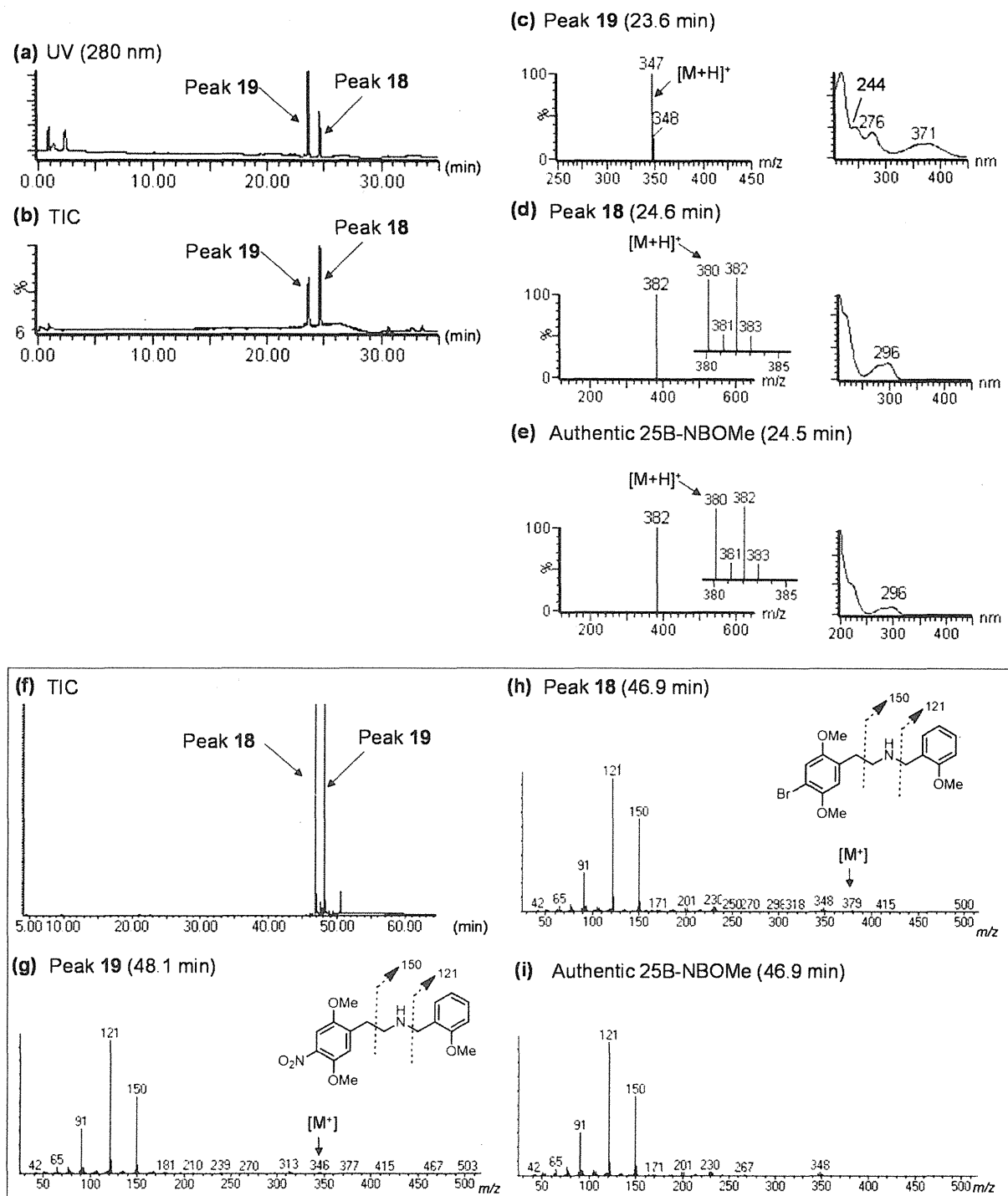


Fig. 15. LC-MS and GC-MS analyses of product L. LC-UV-PDA chromatogram (a) and TIC (b). ESI mass and UV spectra of peaks 19 (c), 18 (d) and authentic 25B-NBOMe (e), respectively. TIC (f) and EI mass spectra of peaks 19 (g), 18 (h) and authentic 25B-NBOMe (i), respectively, obtained by the GC-MS analysis.

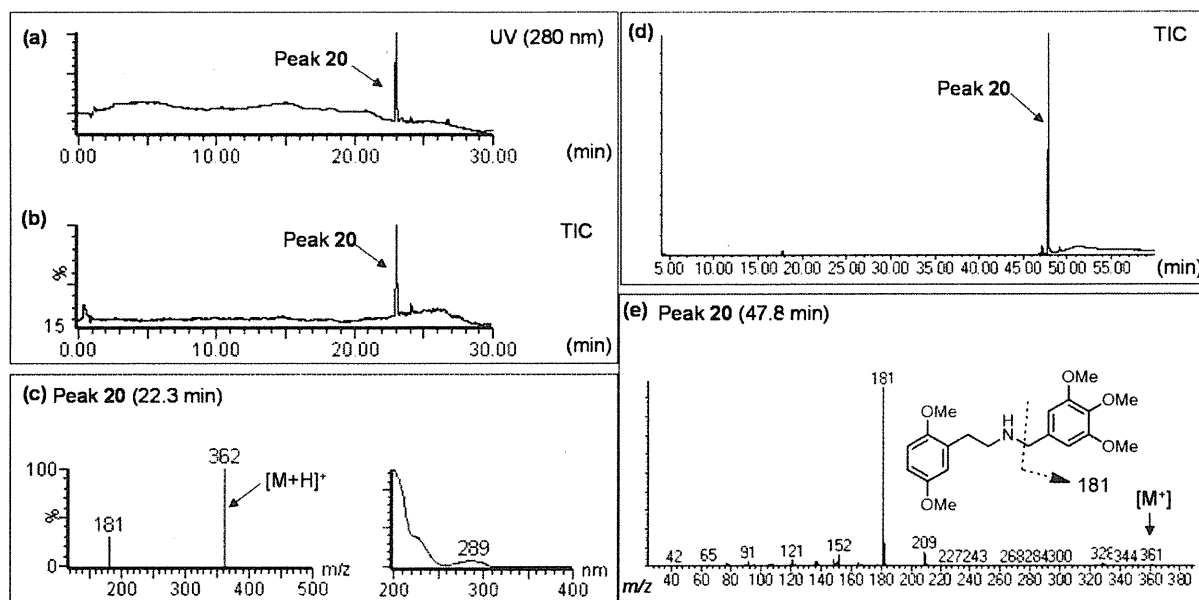


Fig. 16. LC-MS and GC-MS analyses of product M. LC-UV-PDA chromatogram (a) and TIC (b). ESI mass and UV spectra of peak 20 (c). TIC (d) and EI mass spectrum of peak 20 (e) obtained by the GC-MS analysis.

Table 1. NMR data for NNEI (1), 5-Chloro-NNEI (3) and NNEI indazole analog (4)

No.	NNEI (1) ^a		5-Chloro-NNEI (3) ^b		NNEI indazole analog (4) ^a	
	¹³ C	¹³ C	¹ H	¹³ C	¹ H	
1	164.0	163.9	–	160.9	–	
2'	132.3	132.1	7.83, 1H, brs	–	–	
3'	110.9	111.1	–	137.3	–	
3'a	125.5	125.6	–	123.0	–	
4'	122.7	122.8	7.34, 1H, m, overlapped	122.9	8.92, 1H, d, <i>J</i> =8.3 Hz	
5'	121.9	122.0	7.32, 1H, m, overlapped	122.9	7.78, 1H, ddd, <i>J</i> =7.3, 6.9 Hz	
6'	120.1	120.3	8.13, 1H, m, overlapped	126.9	7.91, 1H, td, <i>J</i> =7.3, 0.9 Hz	
7'	110.6	110.5	7.43, 1H, m	109.4	7.93, 1H, brd, <i>J</i> =8.3 Hz	
7'a	136.7	136.7	–	141.1	–	
1''	47.0	46.8	4.20, 2H, t, <i>J</i> =7.2 Hz	49.6	4.93, 2H, t, <i>J</i> =7.3 Hz	
2''	29.6	29.3	1.92, 2H, q, <i>J</i> =7.2 Hz	29.5	2.48, 2H, q, <i>J</i> =7.3 Hz	
3''	29.0	24.2	1.50, 2H, m	29.0	1.86, 2H, m, overlapped	
4''	22.3	32.0	1.80, 2H, q, <i>J</i> =6.9 Hz	22.3	1.83, 2H, m, overlapped	
5''	13.9	44.6	3.51, 2H, t, <i>J</i> =6.9 Hz	14.0	1.37, 3H, t, <i>J</i> =7.3 Hz	
1'''	132.9	132.9	–	132.4	–	
2'''	121.0	121.0	8.08, 1H, d, <i>J</i> =7.2 Hz	119.4	8.79, 1H, d, <i>J</i> =7.3 Hz	
3'''	125.9	125.9	7.52, 1H, m, overlapped	126.0	8.00, 1H, t, <i>J</i> =7.8 Hz	
4'''	125.6	125.6	7.72, 1H, d, <i>J</i> =8.3 Hz	125.0	8.16, 1H, d, <i>J</i> =8.3 Hz	
4'''a	134.2	134.2	–	134.2	–	
5'''	128.8	128.8	7.89, 1H, dd, <i>J</i> =7.6, 1.7 Hz	128.8	8.35, 1H, d, <i>J</i> =7.8 Hz	
6'''	126.0	126.0	7.50, 1H, td, <i>J</i> =6.9, 1.4 Hz, overlapped	125.9	7.98, 1H, ddd, <i>J</i> =7.8, 7.3, 0.9 Hz	
7'''	126.3	126.4	7.53, 1H, td, <i>J</i> =6.9, 1.4 Hz, overlapped	126.2	8.03, 1H, ddd, <i>J</i> =8.9, 8.3, 1.4 Hz	
8'''	120.8	120.9	7.98, 1H, d, <i>J</i> =8.3 Hz	120.5	8.52, 1H, d, <i>J</i> =8.3 Hz	
8'''a	127.4	127.4	–	126.7	–	
NH	–	–	8.12, 1H, brs, overlapped	–	9.90, 1H, s	

^a Recorded in CDCl₃ at 800MHz (¹H) and 200MHz (¹³C), respectively; data in δ ppm (*J* in Hz).

^b Recorded in CDCl₃ at 600MHz (¹H) and 150MHz (¹³C), respectively; data in δ ppm (*J* in Hz).

Table 2. ^{13}C -NMR Data of compounds **6**, **7**, **9** – **11** and α -PVP ^a

No.	α -PVP ^b	α -PHPP (6) ^b	α -POP (7) ^b	4-Fluoro- α -PVP (9) ^b	α -EAPP (10) ^c	<i>N</i> -Ethyl-4-methylpentedrone (11) ^c
1	198.9	198.7	198.7	198.9	196.4	195.8
2	66.8	66.8	66.8	69.3	60.5	60.3
3	32.1	30.1	30.1	31.5	31.8	31.9
4	19.7	25.9	26.2	19.9	17.2	17.2
5	14.2	31.9	29.5	14.3	13.6	13.7
6	–	22.5	31.6	–	–	–
7	–	14.0	22.7	–	–	–
8	–	–	14.1	–	–	–
1'	137.0	136.9	137.0	133.8, d, $J=2.9$ Hz ^d	133.9	131.5
2'/6'	129.2	129.2	129.2	132.1, d, $J=8.7$ Hz ^d	128.7	128.9
3'/5'	129.3	129.3	129.3	115.8, d, $J=21.7$ Hz ^d	129.2	129.8
4'	134.1	134.2	134.2	165.8, d, $J=252.9$ Hz ^d	134.8	145.7
2''/5''	51.2	51.3	51.3	50.6	–	–
3''/4''	24.0	24.0	24.0	23.8	–	–
<i>N</i> -CH ₂ CH ₃	–	–	–	–	41.2	41.2
<i>N</i> -CH ₂ CH ₃	–	–	–	–	11.2	11.2
4'-Me	–	–	–	–	–	21.3

^a Recorded at 600 MHz (^1H) and 150 MHz (^{13}C), respectively; data in δ ppm (J in Hz). ^b Recorded in pyridine-*d*₅.

^c Recorded in DMSO-*d*₆. ^d Observed as double signals by coupling with fluorine.

Table 3. ^1H -NMR Data of compounds **6**, **7**, **9** and **11** ^a

No.	α -PHPP (6) ^b	α -POP (7) ^b	4-Fluoro- α -PVP (9) ^b	<i>N</i> -Ethyl-4-methylpentedrone (11) ^c
1	–	–	–	–
2	5.02, 1H, brs	5.03, 1H, brs	4.88, 1H, brs	5.20, 1H, brs
3	2.09, 2H, m	2.11, 2H, m	2.05, 2H, m	1.85, 2H, m
4	1.35, 2H, m	1.37, 2H, m	1.36, 2H, m	1.27, 1H, m, overlapped 1.05, 1H, m
5	1.09, 2H, m, overlapped	1.12, 2H, m, overlapped	0.77, 3H, t, $J=7.4$ Hz	0.76, 3H, t, $J=7.2$ Hz
6	1.07, 2H, m, overlapped	1.02, 2H, m, overlapped	–	–
7	0.69, 3H, t, $J=7.2$ Hz	1.08, 2H, m, overlapped	–	–
8	–	0.72, 3H, t, $J=7.6$ Hz	–	–
1'	–	–	–	–
2'/6'	8.32, 2H, t, $J=7.6$ Hz	8.33, 2H, dd, $J=8.6, 1.4$ Hz	8.35, 2H, d, $J=8.7$ Hz	7.97, 2H, d, $J=7.9$ Hz
3'/5'	7.49, 2H, t, $J=7.6$ Hz	7.50, 2H, t, $J=8.6$ Hz	7.06, 2H, d, $J=8.7$ Hz	7.41, 2H, d, $J=7.9$ Hz
4'	7.57, 1H, t, $J=7.6$ Hz	7.58, 1H, tt, $J=8.6, 1.4$ Hz	–	–
2''/5''	3.27, 3.08, each 2H, brs	3.28, 3.10, each 2H, brs	3.23, 3.03, each 2H, brs	–
3''/4''	1.79, 4H, m	1.80, 4H, m	1.77, 4H, m	–
<i>N</i> -CH ₂ CH ₃	–	–	–	2.99, 2.89, each 1H, m
<i>N</i> -CH ₂ CH ₃	–	–	–	1.22, 3H, t, $J=7.2$ Hz
4'-Me	–	–	–	2.40, 3H, s

^a Recorded at 600 MHz (^1H) and 150 MHz (^{13}C), respectively; data in δ ppm (J in Hz). ^b Recorded in pyridine-*d*₅.

^c Recorded in DMSO-*d*₆.

Table 4. NMR Data of 3,4-Dichloromethylphenidate (**14**)^a

No.	¹³ C	¹ H
1	170.5	–
2	52.0	4.16, 1H, d, <i>J</i> =8.6 Hz
1'	134.7	–
2'	130.9	7.61, 1H, brs
3'	131.6	–
4'	131.2	–
5'	131.1	7.68, 1H, d, <i>J</i> =8.3 Hz
6'	129.3	7.30, 1H, d, <i>J</i> =8.3 Hz
1''	–	NH 8.90, 1H, brs
2''	56.4	3.83, 1H, brs
3''	25.7	1.41, 1H, m, overlapped 1.26, 1H, q, <i>J</i> =12.7 Hz
4''	21.2	1.67, 1H, t, <i>J</i> =12.7 Hz, overlapped 1.41, 1H, m, overlapped
5''	21.6	1.67, 1H, t, <i>J</i> =12.7 Hz, overlapped 1.54, 1H, q, <i>J</i> =12.7 Hz
6''	44.6	3.26, 1H, brd, <i>J</i> =12.7 Hz 2.93, 1H, t, <i>J</i> =12.7 Hz
1-OMe	53.0	3.67, 3H, s

^a Recorded in DMSO-*d*₆ at 600 MHz (¹H) and 150 MHz (¹³C), respectively; data in δ ppm (*J* in Hz).

Table 5. NMR data for compound **16** and known related compounds

No.	Compound 16 ^{a,b}		2-Acetyl-1-methyl-1 <i>H</i> -benzimidazole ^c	JWH-018 indazole analog ^a
	¹³ C	¹ H	¹³ C	¹³ C
1	188.9	–	193.1	191.6
2'	147.3	–	146.5	–
3'	–	–	–	142.6
3'a	141.8	–	141.5	124.3
4'	122.3	7.87, 1H, d, <i>J</i> =8.3 Hz	121.2	123.1
5'	123.8	7.35, 1H, ddd, <i>J</i> =8.3, 7.2, 1.0 Hz	124.2	123.7
6'	125.9	7.46, 1H, ddd, <i>J</i> =8.3, 7.2, 1.0 Hz	126.3	126.9
7'	110.6	7.51, 1H, m, overlapped	111.3	109.5
7'a	136.1	–	137.3	140.6
1''	45.4	4.70, 2H, t, <i>J</i> =7.6 Hz	31.8 (NMe)	49.8
2''	30.1	2.05, 2H, q, <i>J</i> =7.9 Hz	27.1 (COMe)	29.4
3''	22.8, d, <i>J</i> =4.3 Hz ^c	1.59, 2H, m	–	28.8
4''	30.0, d, <i>J</i> =20.2Hz ^c	1.80 and 1.76, each 1H, m, overlapped	–	22.2
5''	83.7, d, <i>J</i> =164.7 Hz ^c	4.48 and 4.41, each 1H, t, <i>J</i> =5.8 Hz	–	13.9
1'''	134.4	–	–	136.3
2'''	131.9	8.03, 1H, dd, <i>J</i> =7.2, 1.0 Hz	–	129.3
3'''	124.3	7.56, 1H, m, overlapped	–	124.3
4'''	133.3	8.05, 1H, d, <i>J</i> =8.3 Hz	–	131.4
4'''a	134.0	–	–	133.8
5'''	128.6	7.91, 1H, d, <i>J</i> =7.9 Hz	–	128.3
6'''	126.5	7.53, 1H, m, overlapped	–	126.1
7'''	127.9	7.57, 1H, m, overlapped	–	127.1
8'''	125.3	8.46, 1H, d, <i>J</i> =8.3 Hz	–	125.8
8'''a	131.2	–	–	131.1

^a Recorded in CDCl₃ at 600MHz (¹H) and 150MHz (¹³C), respectively; data in δ ppm (*J* in Hz)

^b Observed as double signals by coupling with fluorine

^c [Ref] Lopyrev VA, et al., Org. Magn. Reson. (1982) 20:212–216., recorded in CD₃OD